Nucleic Acids Research, 2025, **53**, gkaf901
https://doi.org/10.1093/nar/gkaf901
Methods

Label-free technique for universal and sequence independent detection of oligonucleotides and nuclease activity

Negin Gooran[1,*], **Baris A. Borsa**[2], **Frank J. Hernandez**[2,3,4], **Harri Härmä**[1], **Kari Kopra**[1]

[1]Department of Chemistry, University of Turku, 20500 Turku, Finland
[2]Department of Physics, Chemistry, and Biology (IFM), Linköping University, 58330 Linköping, Sweden
[3]Department of Bioengineering and Biosciences, TECNUN, Navarra University, 20009 Donostia, Spain
[4]IKERBASQUE, Basque Foundation for Science, 48009 Bilbao, Spain

[*]To whom correspondence should be addressed. Email: negin.gooran@utu.fi

Abstract

Nucleases are a diverse group of enzymes cleaving phosphodiester bonds of deoxyribonucleic acid (DNA) or ribonucleic acid (RNA) with varying specificity. Depending on the context, nucleases can be considered as unwanted contaminants, molecular biology tools, drug targets, or diagnostic markers. Current methods for nuclease activity monitoring are mainly based on fluorescence detection, by using either labeled substrates or oligonucleotide-binding dyes. These methods are often limited to single- and double-stranded DNA or RNA or the determination of either endo- or exonuclease activity. Universal, simple, and sensitive nucleotide sequence and modification-independent methods, enabling endo- and exonuclease activity monitoring, are not currently available. To address this, we have developed the NucleoProbe technique, as a label-free and substrate-independent option for high-sensitivity endo- or exonuclease activity monitoring. External peptide-probe-based detection utilizing time-resolved luminescence readout enables low nanomolar sensitivity for DNA and RNA oligonucleotides down to 9 nt in length. We also demonstrate the universality by monitoring both endo- and exonuclease activity, with over five-fold improved sensitivity in comparison to our commercial standard assay. Additionally, we show the further potential of the method by specifically detecting *S. aureus* via its specific micrococcal nuclease activity and, finally, by monitoring nuclease activity from spiked urine.

Graphical abstract

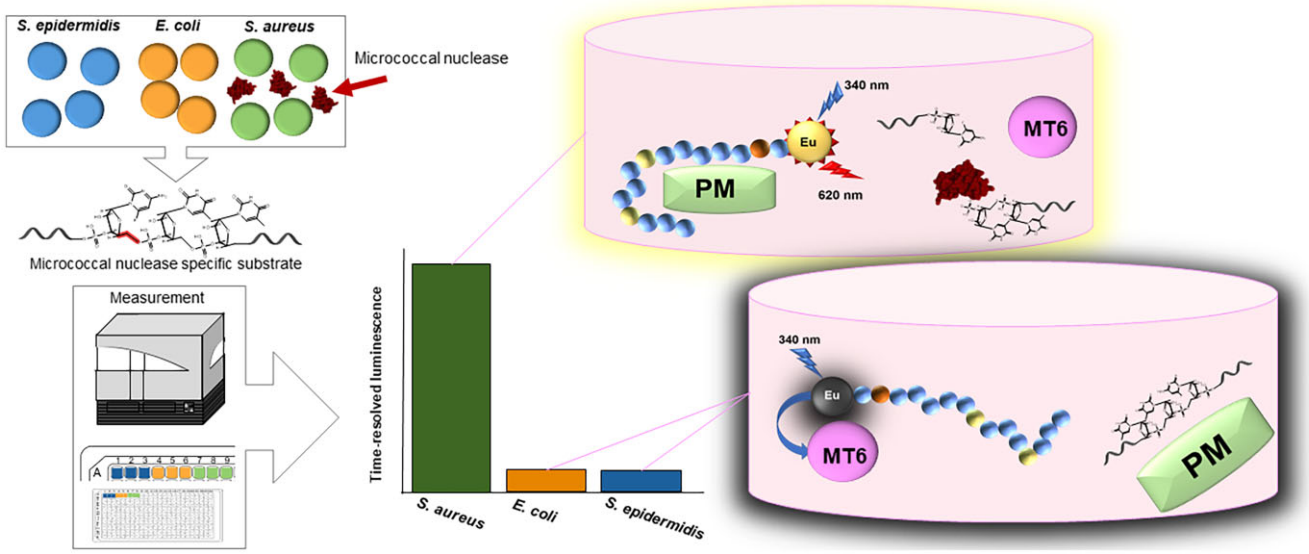

Received: March 12, 2025. **Revised:** August 17, 2025. **Accepted:** August 19, 2025

Introduction

Oligonucleotides are 10–50 nt single- or double-stranded ribonucleic acid (RNA) or deoxyribonucleic acid (DNA) sequences, which are widely used in molecular biology and diagnostics. As an example, techniques such as polymerase chain reaction (PCR), hybridization assays, and microarray techniques utilize either long or short RNA/DNA sequences [1, 2]. Lately, oligonucleotide therapeutics, including small interfering RNA, antisense RNA, microRNA, aptamers, and especially antivirals and vaccine constituent oligonucleotides, have drawn attention [3, 4]. Usually, these oligonucleotide therapeutics contain modified sequences with unnatural nucleotides, to mobilize the oligonucleotide for a specific task, such as selective target recognition, or to increase their stability. In addition, deeper analysis of human diseases on the molecular level during recent decades has led to an increased interest in the quality and quantity of nucleic acids [5]. The important role of oligonucleotides in drug discovery and therapy is the result of almost half a century of developing methods to investigate oligonucleotides [2, 6].

Nucleases are enzymes that cleave phosphodiester bonds of DNA and/or RNA [7, 8]. They are divided into two main categories based on their activity placements. Exonucleases cleave the oligonucleotide from one end to the other end, while endonucleases are restricted to cutting within the polynucleotide sequence. In cells, nucleases play an important role, e.g. in DNA replication, recombination, and RNA interference [9]. Understanding and detecting nuclease activity is the key to uncovering more complex biological mechanisms and diseases such as cancer [10] and autoimmune diseases [11–13]. Even though the gold standard PCR-based methods are the main techniques to be used for the detection of specific nucleic acid sequences through microorganism- or disease-specific nucleic acid amplification process, nuclease activity can be utilized or combined with these methods as an additional biomarker [7, 12, 14–17].

One of the most popular methods to quantify the total nucleic acid concentration is UV absorbance at 260 nm [18, 19]. UV absorbance is a simple and rapid method for quantification, but it lacks sensitivity and cannot provide any other information about the nucleic acid sample, except the concentration. A major drawback is the absorbance overlap between nucleic acids and common contaminants such as proteins [20, 21]. In addition to UV absorbance, fluorescence assays, especially by utilizing oligonucleotide binding and intercalating dyes, are often used especially for longer sequences. These methods are not all well suited for measuring oligonucleotides, but there are many commercially available methods also for short oligonucleotides [22, 23]. For example, Qubit™ offers various commercially available kits for quantification of DNA, RNA, and free nucleotides, based on the use of different fluorescent dyes [24–26]. These methods are compared in a more detailed fashion in Supplementary Table S1.

There are several methods for detecting nuclease activity based on fluorometric, electrochemical, or colorimetric detection (Supplementary Table S2). In general, fluorescent-based methods offer a relatively high sensitivity and user-friendly protocols for activity measurements [7, 27]. Fluorescence resonance energy transfer (FRET)-based probes are one of the most commonly used tools for detecting nuclease activity [12, 28]. One of the main limitations of these methods is, however, the use of two usually covalently attached dyes, donor and acceptor, to the substrate oligonucleotide [29]. This complicates the change of the substrate sequence and also limits its use only for endonucleases. Some of the commercially available kits are based on a single oligonucleotide-conjugated environment-sensitive fluorophore, such as fluorescein (FAM). These assays rely on the changes in FAM environment upon oligonucleotide degradation by the nuclease, detected as a change in fluorescence signal [30]. Also, this type of method has limited usability, often enabling detection only for endonuclease activity. Currently, there are limited options for the detection of nuclease activity without a specific substrate oligonucleotide using external dyes. These assays typically rely on nucleic acid-binding dyes, but their sensitivity often depends on the length of the target sequence, compromising the usability of short oligonucleotides [31, 32].

For years, our group has developed methods for biomolecule detection, mainly based on lanthanide chelates and time-resolved luminescence (TRL). We have previously shown that Eu^{3+} nanoparticles can detect oligonucleotides, through competition between nucleic acids and protein adsorption on labeled nanostructures [33]. We have also introduced the Protein-Probe technique, for protein stability and interaction monitoring, utilizing an external peptide probe (Eu^{3+} probe) [34–36]. Oligonucleotides are not detected with the Protein-Probe, but these two works served as an inspiration for a novel technique called the NucleoProbe, reported here. This three-component method is based on the use of a protein-derived positive modulator, which produces a measurable TRL-signal with the Eu-probe in the modulator solution, in the absence of oligonucleotide (Fig. 1) [36]. Upon addition of the target oligonucleotide, a low TRL-signal is observed due to competition between the nucleic acids and the protein for binding to the Eu-probe. We show that the NucleoProbe can detect 9–60 nt single-stranded (ss) and double-stranded (ds) DNA and RNA with the same low nanomolar sensitivity, and in an oligonucleotide-sequence-independent manner. We also demonstrate the detection of micrococcal nuclease (MNase) and ribonuclease A and I (RNase A and I) activity in endo- and exonuclease format. Finally, we demonstrate the broader applicability of the NucleoProbe by detecting *Staphylococcus aureus* via its specific MNase activity [37] in bacteria growth media and urine.

Materials and methods

Materials and instrumentation

The nine-dentate Eu^{3+}-chelate, {2,2′,2″,2‴-{[4′-(4‴-isothiocyanatophenyl)-2,2′,6′,2″-terpyridine-6,6″-diyl]bis(methylene-nitrilo)}tetrakis(acetate)}europium(III), and the negative modulator, MT6, were purchased from QRET Technologies (Turku, Finland). The chelate conjugation and the purification of the Eu-probe peptide, H_2N-EYEEEEEVEEEVEEE from Pepmic Co., Ltd (Suzhou, China) were performed as described before [36]. MNase, deoxyribonuclease I (DNase I), S1 nuclease (S1), exonuclease III (Exo III), exonuclease I (Exo I), *haemophilus influenzae* Rd (HindIII), ribonuclease I (RNase I), ribonuclease A (RNase A), tryptone soy agar with 5% defibrinated sheep blood, and Tryptone Soy Broth (TSB) were purchased from Thermo Fisher (Waltham, MA). *Staphylococcus aureus*, *Staphylococcus epidermidis*, and *Escherichia coli* were obtained from

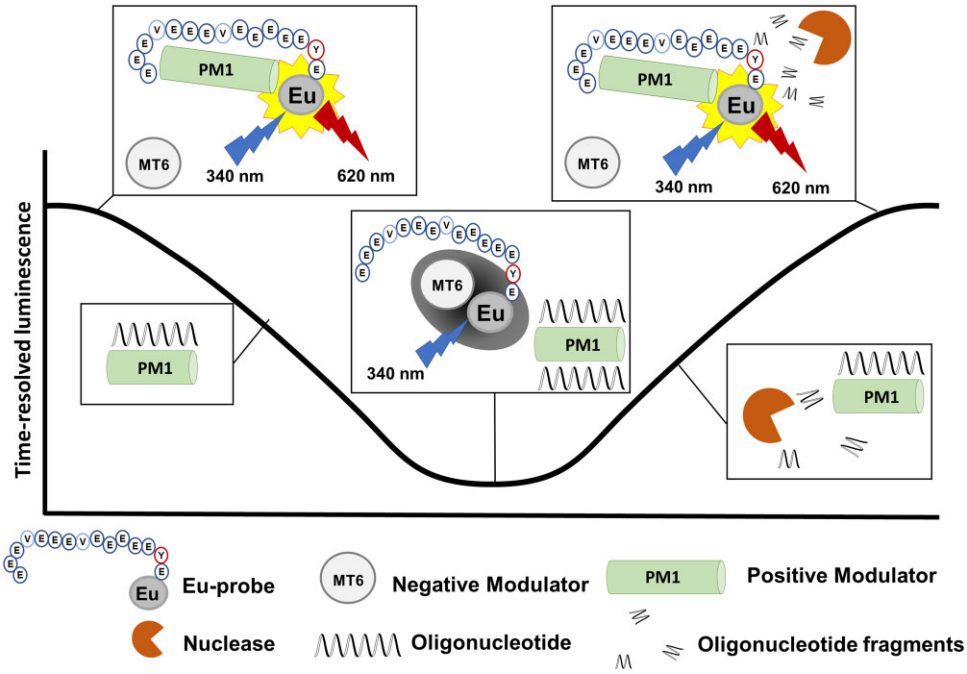

Figure 1. Oligonucleotide concentration and nuclease activity monitoring using the NucleoProbe technique. At low oligonucleotide concentration, the positive modulator interacts with the Eu-probe resulting in high TRL-signal. Increasing concentration of oligonucleotide prevents this interaction, and the negative modulator decreases the Eu-probe signal. Degradation of oligonucleotide by nuclease improves the accessibility of the positive modulator to the Eu-probe, thus increasing the TRL-signal.

Linköping University (Linköping, Sweden). The urine samples were collected from four healthy and volunteer individuals, with written informed consent from each participant. The study setting was consulted by the local Turku Clinical Research Centre, which did not require official ethical approval. All assays were performed on white, nonbinding, low-volume 384-well assay plates (Corning Inc., Kennebunk, ME). All used oligonucleotides were purchased from biomers.net (Ulm, Germany) (Table 1). DNase I Detection Kit (DD Kit) (Cat. No. PP-410S) was purchased from Jena Bioscience (Jena, Germany). All other reagents, including basic buffer reagents, solvents, 1,1′,3,3,3′,3′-hexamethylindodicarbocyanine iodide (HIDC), carbonic anhydrase from bovine erythrocytes (PM1), bovine serum albumin (PM2), and RNase-free water, were purchased from Sigma–Aldrich (Darmstadt, Germany or St. Louis, MO).

The NucleoProbe detection solution (DS) consists of 4.1 mM citric acid, 7.9 mM of disodium hydrogen phosphate (pH 4), 0.01% Triton X-100 with signaling components, MT6 (5–12 μM), and Eu-probe (0.5 or 1 nM). Tris+/+, used for oligonucleotide and nuclease activity detection, contains 10 mM Tris–HCl (pH 7), 1 mM $MgCl_2$, and 1 mM $CaCl_2$. The reaction buffers for nuclease are (i) 10 mM Tris–HCl (pH 8.5), 10 mM NaCl, and 1 mM $MgCl_2$ (DNase I); (ii) 4.1 mM citric acid, 7.9 mM disodium hydrogen phosphate (pH 4), 2 mM $ZnCl_2$, and 50 mM NaCl (S1); (iii) 10 mM Tris–HCl (pH 7.5), 10 mM $MgCl_2$, and 1 mM dithiothreitol (DTT) (pH 7) (ExoIII); (iv) 10 mM Tris–HCl (pH 7.5), 5 mM $MgCl_2$, and 5 mM NaCl (HindIII); and (v) 67 mM glycine–KOH (pH 9.5), 5 mM $MgCl_2$, and 1 mM TT (ExoI).

Nuclease reaction incubations were performed using PTC-100 Programmable Thermal Controller (MJ Research, Inc., Watertown, MA), with the exception of those at room temperature (RT). TRL and fluorescence measurements were performed using Spark 20M from Tecan Life Sciences (Männedorf, Switzerland). TRL-signals were monitored using excitation at 340 and emission at 620 nm wavelengths and 800 and 400 μs delay and decay times, respectively.

NucleoProbe technique development for oligonucleotide detection

All assays were performed in biological triplicate using 5 μl sample and 15 μl DS volumes. All individual experiments were repeated at least three times, unless otherwise indicated. Concentrations are reported in relation to the sample or DS volumes. PM1 and PM2 were prepared at 100 μM concentration in milli-Q water and PM1 was further activated at 10 μM concentration by incubating at 75°C for 5 min. PM1 preactivation was studied, and PM1 and PM2 concentrations (0.12–2000 nM) were optimized using DS (7.5 μM MT6 and 0.5 nM Eu probe) in 20 μl volume. In all cases, TRL-signals were measured at several points during 60-min incubation after DS addition. Using the selected concentrations for PM1 (5 nM) and PM2 (20 nM), oligonucleotide titration using Sc1 (1–1000 nM) and DS (7.5 μM MT6 and 0.5 nM Eu probe) was performed. The signal stability of PM1 after preactivation was studied using 20 nM PM1 and 300 nM Sc1 from Day 0 (preactivation day) to Day 6. The preactivation cycles were performed at 24 h, 48 h, or 6-day intervals. The TRL-signals used in the figures were monitored after 5 min of incubation after DS addition.

All oligonucleotides were dissolved in milli-Q water (500 μM), and dsDNA hybridization (100 μM) was performed in 50 mM Tris (pH 7.5), and 50 mM NaCl by incubating at 85°C for 3 min followed by slow cooling. Oligonucleotide detection was performed by adding the tested oligonucleotide (0.02–4800 nM, Table 1) in Tris+/+ (3 μl), followed by 5 nM PM1

Table 1. Oligonucleotides used in this work

Name	Length (nt)	Sequence
T6	6	5′-ttt ttt-3′
T7	7	5′-ttt ttt t-3′
T8	8	5′-ttt ttt tt-3′
T9	9	5′-ttt ttt ttt-3′
T12	12	5′-ttt ttt ttt ttt-3′
T15	15	5′-ttt ttt ttt ttt ttt-3′
Sc20	20	5′-cac tac taa gct tta gct ac-3′
Sc40	40	5′-cac tac taa gct tta gct acc act act aag ctt tag cta c-3′
Sc60	60	5′-cac tac taa gct tta gct acc act act aag ctt tag cta cca cta cta agc ttt agc tac-3′
Sc8	8	5′-cac tac ta-3′
Sc8ds[a]	8	5′-cac tac ta-3′ and 5′-tag tag tg-3′
Sc9	9	5′-cta agc ttt-3′
Sc9ds[a]	9	5′-cta agc ttt -3′ and 5′-aaa gct tag-3′
Sc9Cds[a]	9	5′-gat tcg aaa-3′ and 5′-aaa gct tag-3′
Sc12	12	5′-cta agc ttt agc-3′
Sc12ds[a]	12	5′-cta agc ttt agc -3′ and 5′-gct aaa gct tag-3′
Sc12Cds[a]	12	5′-gat tcg aaa tcg-3′ and 5′-gct aaa gct tag-3′
Sc1	12	5′-atg tcg cac atg-3′
Sc1ds[a]	12	5′-atg tcg cac atg -3′ and 5′-cat gtg cga cat-3′
Sc2	15	5′-atg tcg cac atg tcg-3′
Sc2ds[a]	15	5′-atg tcg cac atg tcg-3′ and 5′-cga cat gtg cga cat-3′
A15	15	5′-aaa aaa aaa aaa aaa-3′
Sc2c	15	5′-cga cat gtg cga cat-3′
ATT15	15	5′-att att att att att -3′
GCC15	15	5′-gcc gcc gcc gcc gcc-3′
Sc15	15	5′-ggt tgg tgt ggt tgg-3′
Sc15Bio	15	5′-ggt tgg tgt ggt tgg -biotin[b]
RNA12	12	5′-cgc uac aau cgc-3′
TTFx	11	5′-mUmUmU mUtt FxmUmU mUmU-3′[c]
FxTT	11	5′-mUmUmU mUFxt tmUmU mUmU-3′
Fx Control	9	5′-mUmUmU mUFxmU mUmUmU-3′

[a]double-stranded DNA
[b]3′ terminus: Biotin-TEG
[c]mU: 2′-*O*-methyl uridine, T: DNA thymidine, Fx: floxuridine [37]

(2 μl). After a quick shake, 15 μl optimized DS was added, and TRL-signals were monitored after 5 min of incubation.

Nuclease activity monitoring with nucleoprobe

The nuclease assays were performed by using 10 nM substrate oligonucleotide (1 μl). MNase, DNase I, and S1 nuclease reactions were performed with Sc1, Exo III and Exo I reactions with Sc8, Sc8ds, Sc12, and Sc12ds, HindIII reactions were performed using Sc9ds, Sc9Cds, Sc12ds, and Sc12Cds, and RNase I and RNase A reactions were performed using Sc1 and RNA12 (Table 1). In each case, nuclease (6–25 000 μU) was added in 3 μl using nuclease-specific reaction buffer. Reactions were incubated for 30 min at 37°C, prior to PM1 (5 nM) addition (1 μl). Thereafter, 15 μl of DS was added, and TRL signals were monitored as previously.

The NucleoProbe parameters were optimized for the 1:400 diluted TSB by testing varying concentrations of MT6 (5–7.5 μM), Eu probe (0.5 or 1 nM), PM1 (10–30 nM), and Sc12 (5–100 nM). The spiked TSB samples were tested by incubating (30 min at 37°C) 10 nM of Sc12 or 5 nM of TTFx (1 μl), with 3 μl of the diluted MNase (1.5–6250 μU) in diluted TSB. PM1 (5 nM) was added in 1 μl, followed by DS (5 μM of MT6 and 0.5 nM of Eu probe) addition in 15 μl, and TRL-signal measurement as previously.

The NucleoProbe parameters were optimized for studying 1:100 diluted urine samples in 1 mM $CaCl_2$-supplemented water, using varying concentrations of MT6 (5–12 μM), Eu-probe (0.5 or 1 nM), and PM1 (5–50 nM). Assay parameters of 12 μM MT6, 1 nM Eu probe, 20 nM PM1, and 20 nM Sc12 were chosen for studying urine samples, measured at several time points 5–90 min. Nuclease assays in urine were performed by spiking the urine with MNase (0.06–4000 μU). Sc12 and TTFx (20 nM) were added in 1 μl and mixed with 1:100 diluted spiked urine (3 μl, 1 mM $CaCl_2$). Reactions were incubated for 30 min at 37°C, followed by the addition of 20 nM PM1 (1 μl), 15 μl of DS (12 μM of MT6 and 1 nM of Eu-probe), and TRL-signal monitoring after 5 min of incubation.

Nuclease activity monitoring using DNase Detection Kit

DD Kit was used according to the manufacturer's instructions. Briefly, MNase (0.25–40 000 μU/well) or DNase I (6–100 000 μU/well) was mixed with an equal volume (10 μl) of DNase Detection Master. Reactions were incubated for 30 min at 37°C, prior to fluorescence measurement at RT. The fluorescence signal was measured with 485 nm excitation and 530 nm emission wavelengths.

Identification of *S. aureus* based on its nuclease activity using the nucleoprobe

Bacterial cultures were performed as previously described [37]. Briefly, bacteria were inoculated onto tryptone soy agar with 5% defibrinated sheep blood, and incubated for 24 h at 37°C. A single colony was transferred to 25 ml TSB (50 ml autoclaved glass Erlenmeyer) and incubated for 24 h at 37°C with shaking at 120 rpm. Fifty microliters of the liquid cultures were diluted in 25 ml fresh TSB (50 ml autoclaved glass Erlenmeyer) and incubated under the same conditions for 12 h. Supernatants for nuclease activity assays were collected and centrifuged at 4500 × *g* for 30 min. Supernatants were diluted in Tris+/+ buffer to 1:400, 1:800, 1:1600, and 1:3200. The NucleoProbe assay was performed as previously by incubating 10 nM of Sc12 or 5 nM of TTFx, FxTT, or Fx Control (1 μl), with 3 μl of the diluted supernatant for 30 min at 37°C. PM1 (5 nM) was added in 1 μl, followed by DS (5 μM of MT6 and 0.5 nM of Eu probe) addition in 15 μl, and TRL-signal measurement after 5 min of incubation.

Data analysis

μ_{max}/μ_{min} represents the signal-to-background ratio (S/B). Coefficient of variation (CV%) was calculated as $(\sigma/\mu) \times 100$, where μ is the mean value and σ is the standard deviation (SD). The effective concentration (EC_{90} or EC_{10}) and half-maximal effectivity concentration (EC_{50}) were calculated from standard sigmoidal fitting functions (Logistic) using Origin 2016 (OriginLab, Northampton, MA) software.

Results

The NucleoProbe technique is based on the Eu-probe, Eu^{3+} chelate conjugated negatively charged peptide, and its TRL-signal modulation in the presence or absence of oligonucleotides (Fig. 1). In the absence of oligonucleotide, the Eu-

probe interacts with the PM, protecting the Eu^{3+}-chelate from quenching by the negative modulator, and produces a high TRL signal [36]. In the presence of oligonucleotide, interaction between PM and the Eu-probe is blocked due to the competitive binding with the oligonucleotide, allowing the negative modulator to quench the TRL-signal. Nuclease activity restores the PM interaction with the Eu-probe by cleaving the oligonucleotide and reducing its affinity, thus restoring the high TRL-signal monitored (Fig. 1).

NucleoProbe detects oligonucleotides in a length-dependent manner, independent of their sequence and single- or double-stranded nature

The NucleoProbe was developed by first introducing the PM and thereafter by optimization of the used negative modulator. This was based on the Protein-Probe protein thermal-stability assay as our starting point [34, 36]. In the original Protein-Probe assay, HIDC (negative modulator) and the Eu-probe were the key components for detection at pH 4, but this setting is unsuitable for oligonucleotide detection. Thus, we started by introducing an additional component, a positive modulator, and screened a preselected set of both positive and negative modulators in varying combinations with the Eu-probe (0.25–2 nM). Based on these screenings, we selected MT6 (7.5 μM) as our negative modulator to use with the 0.5 nM Eu-probe, to further evaluate two positive modulators (PM1 and PM2) (Supplementary Fig. S1). As we found that the PM1 benefits from heat activation (5 min at 75°C), this step was performed prior to its use, while PM2 was used without the preactivation step. Under these conditions, EC_{50} values of 20 ± 1.3 and 426 ± 39 nM were detected for PM1 and PM2, respectively. The maximal TRL-signals for PM1 and PM2 were saturated approximately at the same order of magnitude of TRL-signal, but PM1 was detectable at lower concentration compared to PM2 (Supplementary Fig. S1). We expected the PM concentration to directly correlate with the oligonucleotide detection sensitivity, and tested this hypothesis by using varying concentrations of PM1 and PM2 in Sc1 titration. By setting S/B 5 as our cutoff, we observed that ∼2-fold higher DNA concentration is needed in comparison to the used PM concentration in both cases. With the minimum PM1 (5 nM) and PM2 (20 nM) concentrations, the cutoff was reached with ∼10 and 50 nM DNA, respectively (results not shown). Based on this, PM1 (5 nM) was selected to be used, and thus, we further studied its preactivation. Our results indicate that once PM1 is activated, it produces a sufficiently stable TRL-signal for 96 h (Supplementary Fig. S2). Thereafter, a dramatic TRL-signal decrease is observed, but it can be prevented by repeating the activation steps, which can be performed for a maximum of 10 times for the same PM1 batch (Supplementary Fig. S3). Multiple reactivation cycles reduce the TRL-signal produced by PM1, but it maintains assay functionality despite a reduced S/B ratio. This means that the lifetime of one PM1 batch can be increased by at least a month, if needed, after the first activation, by using a 6-day reactivation cycle (Supplementary Fig. S4).

Once the assay conditions were selected, NucleoProbe was used to investigate DNA oligonucleotides with different lengths (6–60 nt), single- or double-stranded nature, and varying sequence (Table 1). Under the selected assay conditions, nanomolar detection of DNA was achieved with DNA sequences over 8 nt (Fig. 2A). The 8 nt long sequence was already clearly less detectable than longer DNA, which gives us an indication of the demands related to nuclease substrate selection. When 9–15 nt DNA sequences were used, nearly equal EC_{50} values (1.0–2.5 nM) were detected, as the longer sequences (20–60 nt) provided slightly lower EC_{50} values (0.6–1.3 nM), respectively (Fig. 2B). Next, we studied ss- and dsDNA, and found that dsDNA has slightly improved detectability independently of its sequence length (9–15 nt) (Fig. 2C). Finally, we found no sequence dependence by using six different sequences (15 nt) with the NucleoProbe, all detectable at low nanomolar concentration (Fig. 2D). In addition, the potential effect of secondary structure, specifically G-quadruplex formation, was tested using a thrombin aptamer, but no changes in detectability were observed [38, 39] (Supplementary Fig. S5).

NucleoProbe enables universal nuclease activity monitoring of endo- and exonucleases

Nucleases are a highly varying set of enzymes having different demands for their buffer and oligonucleotide substrate sequences. Screening system possessing the capability to address the following features would be highly desirable: (i) endonuclease activity protection at both ends; (ii) exonuclease activity detection using non-capped DNA or RNA; (iii) 5′-exonuclease activity protection at the 3′-end; and (iv) 3′-exonuclease activity protection at the 5′-end. To demonstrate the universal nature of the NucleoProbe platform, MNase, DNase I, S1, HindIII, Exo I, and Exo III with ss- and/or dsDNA were studied.

MNase, DNase I, Exo III, and S1 were first titrated, by using Sc1 in an ss form or in the case of Exo III in a dsDNA form. MNase, DNase I, and S1 are all endonucleases, and with the used DNA sequence, all performed quite equally showing μU level detectability (Fig. 3A). Exo III is an exonuclease, and in the assay, it produced an improved S/B ratio but slightly lower sensitivity in comparison to MNase and DNase I. The EC_{50} values for MNase, DNase I, S1, and Exo III are 0.2 ± 0.1, 1.2 ± 0.4, 0.5 ± 0.1, and 2.3 ± 0.7 mU/well, respectively (Fig. 3A). The difference in nuclease functionality was expected; thus, the same sequence was used for both endo- and exo-functional enzymes and without a thorough optimization of the reaction conditions. HindIII restriction enzyme was tested with four different substrates, containing (Sc9ds and Sc12ds) or lacking (Sc9Cds and Sc12Cds) a specific cleaving site (Fig. 3B). NucleoProbe detected the activity of HindIII with Sc9ds with the EC_{50} value of 1.8 ± 0.1 mU/well. Although Sc12ds has the same cleaving site, activity of HindIII was not detected as the product formed from the Sc12ds cleavage was 9 nt and still as detectable at low nanomolar concentrations as the original Sc12ds substrate (Supplementary Fig. S6).

To further confirm the correct functionality of the NucleoProbe nuclease detection, we tested MNase for its dependency on the presence of Ca^{2+}, as its activity is known to be significantly dropped in ion-deficient conditions [40]. We also used EDTA-supplemented Tris buffer, and MNase activity was clearly observed to be drastically reduced in the absence of Ca^{2+} (Supplementary Fig. S7). As a second control experiment, we demonstrate that Exo I (ssDNA-specific exonuclease) and Exo III (dsDNA-specific exonuclease) can efficiently cleave only the used ssDNA or dsDNA specific to their activity (Fig. 3C). The results showed that the EC_{50} values calculated

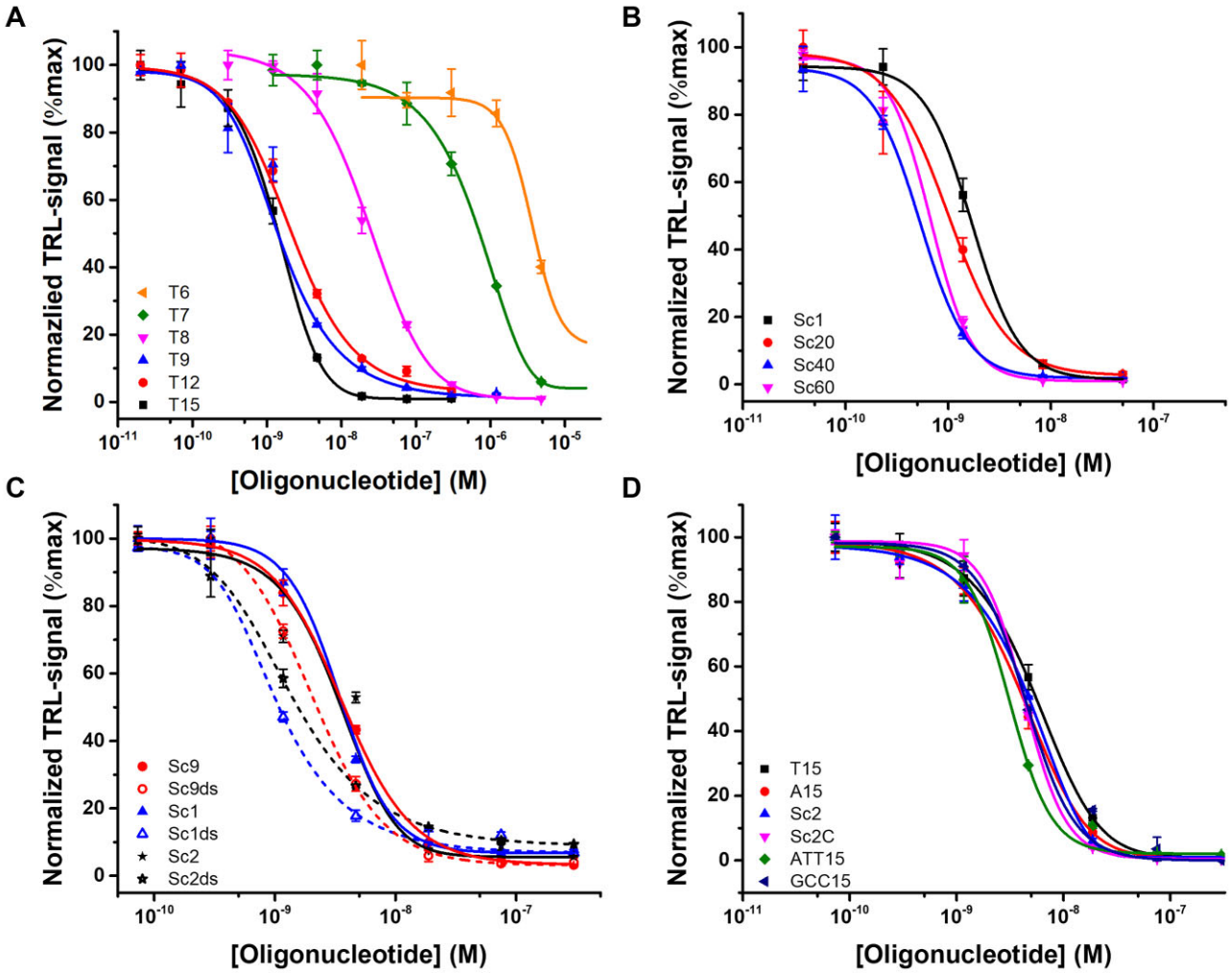

Figure 2. NucleoProbe distinguishes ss- and dsDNA oligonucleotides by length, independent of sequence. DNA titrations (0.02–4800 nM) were performed with both ss- and dsDNA having different length (6–60 nt) and sequence. In a titration with 6–15 nt DNA, sequences over 9 nt were equally detected (**A**), and DNA detectability was only slightly increased with even longer (20–60 nt) DNA sequences (**B**). When ss- and dsDNA were compared (9–15 nt), dsDNAs displayed lower detection limits (**C**), but no clear ssDNA sequence dependence was detected (**D**). All data are presented as mean ± SD.

for both nucleases increase with the length of the substrate. The EC_{50} values of Exo I with Sc8 and Sc12 are 305 ± 14 and 1250 ± 187 μU/well, respectively, and the EC_{50} values of Exo III with Sc8ds and Sc12ds are 226 ± 16 and 2040 ± 261 μU/well, respectively. As expected, Exo I showed no activity with double-stranded substrates and Exo III with single-stranded substrates. Exo I was tested further with Sc15 and Sc15Bio, with 3′-end biotinylation to block exonuclease activity (Supplementary Fig. S8). As expected, Exo I cleaved Sc15, while no activity with Sc15Bio was observed. MNase, used as a control endonuclease, exhibited capping-independent activity with EC_{50} values of 1.1 ± 0.4 and 1.2 ± 0.2 mU/well for Sc15 and Sc15Bio, respectively.

We then compared the NucleoProbe to the DD Kit manufactured by Jena Bioscience (DD Kit) in parallel by using MNase and DNase I (Fig. 3D). The EC_{10} values for DNase I using the DD Kit were 13 ± 1.9 μU/μl (250 ± 38 μU/well), which are in agreement with the values given by the manufacturer and confirm its correct functionality. When the results from the two assays are compared, EC_{50} values for MNase and DNase I using the DD Kit were 1.5 ± 0.9 and 6.8 ± 2.7 mU/well, while for the NucleoProbe they were 0.18 ± 0.01 and 1.9 ± 0.1 mU/well, respectively (Fig. 3D). Finally, we tested the activity of RNase I and RNase A with RNA12 and Sc1 as substrates to demonstrate the ability of NucleoProbe to detect RNA and RNase activity (Supplementary Figs S9 and S10). NucleoProbe showed the same level of sensitivity for RNA as DNA detection (Supplementary Fig. S9). The results indicated that RNase I and RNase A only degraded RNA12, with EC_{50} values of 732 ± 42 and 318 ± 31 μU/well, respectively. MNase, used as the control nuclease, degraded both RNA12 and Sc1 with the EC_{50} of 153 ± 24 and 123 ± 37 μU/well, respectively.

The presence of *S. aureus* can be detected based on its MNase activity using the NucleoProbe technique

Previously, a modified oligonucleotide, containing -TT- as MNase-specific substrate, has been introduced for *S. aureus* identification, based on the MNase secreted by the bacteria [37]. We decided to use this oligonucleotide substrate (TTFx) for our next assays to evaluate the performance of Nucleo-

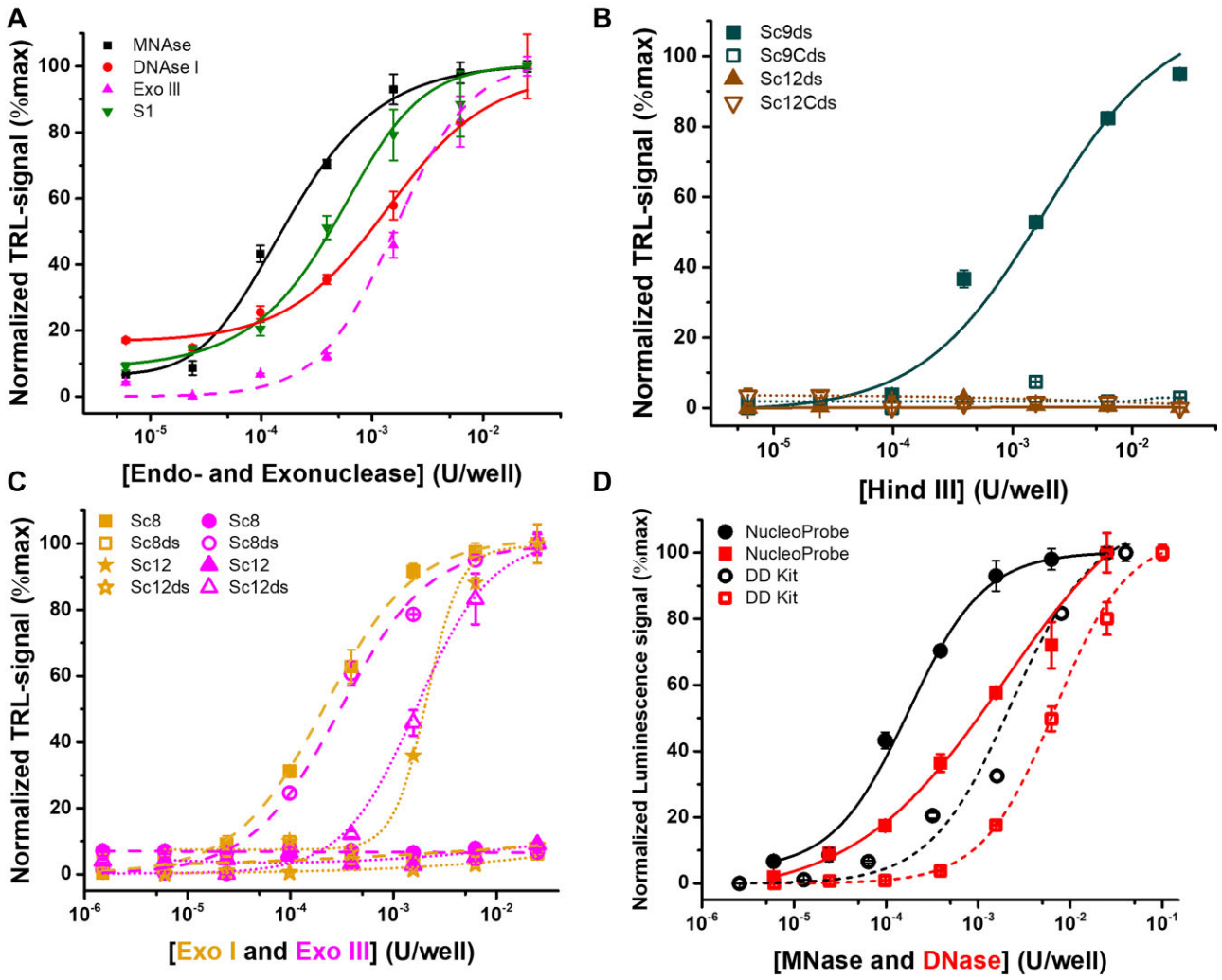

Figure 3. NucleoProbe enables universal detection of both endo- and exonucleases. (**A**) Titration (6–25 000 μU) of different endonucleases (solid line) and exonucleases (dashed line) with 10 nM DNA substrate (Sc1) using the NucleoProbe. (**B**) Titration of the HindIII (6–6250 μU) with 9 nt and 12 nt substrates with (solid line) or without (dotted line) a specific cleavage site. (**C**) Titration of Exo I and Exo III (1.5–25 000 μU) with ssDNAs (dashed line) and dsDNAs (short dashed line). (**D**) Titration (2.6–100 000 μU) of MNase and DNase I using the NucleoProbe (solid line) with Sc1 (10 nM) substrate, and the commercial DD Kit (dashed line). All data are presented as mean ± SD.

Probe in more complex matrixes, to further highlight its suitability for nuclease activity monitoring.

As we moved from the pure buffer conditions to a more complex environment, MT6 and Eu-probe concentration and the dilution used for the NucleoProbe were first evaluated. Bacterial culture media (TSB) was shown to have a quenching effect on the Eu-probe TRL-signal, but the assay functionality was restored by using increased PM1 (10 nM) and decreased MT6 concentration (5 μM) in comparison to buffer conditions (Fig. 4A). In these conditions, S/B ratio over 5 (the set cutoff) was detected with a 1:400 or higher TSB dilution. To enable specific *S. aureus* detection, we first tested the detectability of the modified oligonucleotides selected for MNase activity assay, using the NucleoProbe assay (Supplementary Fig. S11). All the modified sequences (TTFx, FxTT, and Fx control) had slightly improved detectability (average EC_{50} of 1.1 ± 0.2 nM) over the non-modified DNA substrate with similar length (Fig. 2A and Supplementary Fig. S5), which allowed the use of 5 nM substrate also in 1:400 diluted TSB. This, however, had no significant impact on MNase activity monitoring, as Sc12 (10 nM) and TTFx (5 nM) were nearly equally detected, showing EC_{50} values of 164 ± 37 and 178 ± 18 μU/well, respectively (Fig. 4B).

We next continued to prove the specificity of the TTFx cleavage using the NucleoProbe, by using supernatants from the *S. aureus* (positive control), *S. epidermidis* (negative control 1), and *E. coli* (negative control 2) cultures. All three supernatants were tested in four dilutions (1:400–1:3200) and with the TTFx, which was specifically cleaved only in the presence of *S. aureus* MNase (Fig. 4C). As expected, dilution of the supernatants decreased the visibility of the substrate due to the decrease in matrix complexity, and by using dilution over 1:1600, MNase activity is not anymore detectable expectedly due to its low concentration. In any of the given conditions, *E. coli* and *S. epidermidis* showed no detectable signal change, proving the specificity of the assay and the used TTFx substrate (Fig. 4C). All supernatants were also tested using three dilutions (1:400, 1:800, and 1:1600) and Sc12 as a nonspecific nuclease substrate (Supplementary Fig. S12). The results confirmed the presence of the nucleases in all supernatants, and as seen also from Fig. 4C, the visibility of the supernatants' activity decreases with higher dilutions. As an exception, *S. aureus*

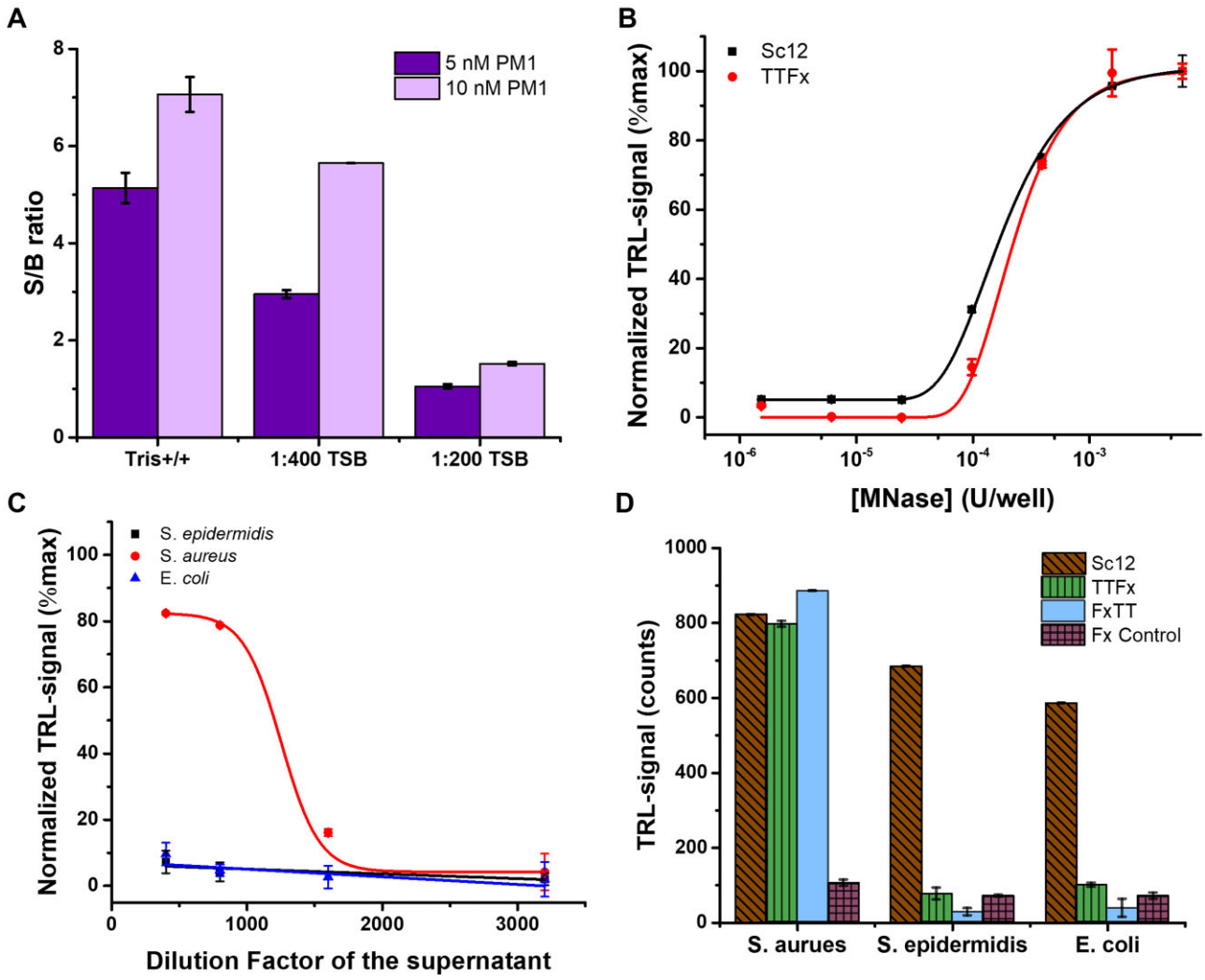

Figure 4. NucleoProbe can specifically detect *S. aureus* based on its MNase activity. (**A**) Sc12 (10 nM) detectability in buffer (Tris+/+) and with 1:400 and 1:200 diluted TSB using 5 μM MT6 and 0.5 nM Eu probe with 5 or 10 nM PM1. (**B**) Titration of MNase (1.5–25 000 μU) in diluted TSB (1:400) with Sc12 (10 nM, black) and TTFx (5 nM) using 5 nM PM1. (**C**) Titration (1:400–1:3200) of three bacterial supernatants, *S. epidermidis*, *E. coli*, and *S. aureus*, with TTFx (5nM). (**D**) Total and MNase-specific nuclease activity in 1:400 diluted supernatants using three bacterial strains and four different substrates, serving as positive (Sc12) and negative (Fx Control) controls, and MNase-specific substrates (TTFx and FxTT). All data were displayed as mean ± SD.

total nuclease activity remained high even with a 1:1600 dilution (Supplementary Fig. S12).

Diluted bacterial supernatants (1:400) were further studied with four different substrates, Sc12 (10 nM) or TTFx, FxTT, and Fx Control (5 nM) (Fig. 4D). Sc12 served as a positive control, which is expected to be cleaved by nearly any nuclease present (Supplementary Fig. S12), while Fx Control is a negative control, expected not to be cleavable by any nuclease. TTFx and FxTT are both MNase specific [37], thus expected to be cleaved only by *S. aureus*. As expected, Sc12 was cleaved by all three bacterial supernatants at the same rate, as Fx Control showed no clear cleavage, and a low TRL-signal was detected in all cases (Fig. 4D). On the other hand, TTFx and FxTT were found equally desirable substrates for *S. aureus* MNase, not cleaved by any other nuclease present in either *E. coli* or *S. epidermidis* supernatants (Fig. 4D). The result was further confirmed by monitoring *S. aureus* MNase activity in Ca^{2+}-free conditions, in which no TTFx cleavage was monitored (Supplementary Fig. S13). As the control DNA (Sc12) was only slightly affected under these conditions, results prove the assay specificity (Fig. 3B and Supplementary Fig. S13) [41].

Nuclease activity can be detected in urine using the NucleoProbe technique

As NucleoProbe was successfully applied to bacterial cultures, we next studied its functionality using MNase-spiked urine. Again, we started by testing the matrix effect using four different urine samples from four different healthy individuals (Fig. 5A). Based on this initial testing, we saw variance in functionality of the NucleoProbe when different 1:100 diluted urine samples were tested. However, all samples were found functional in a condition with 1 nM Eu probe, 25 nM PM1, 12 μM MT6, and 50 nM Sc12. As different urine samples caused different variations in signal, due to their different protein and oligonucleotide concentrations, we selected moderately functional Urine 3, for further NucleoProbe testing. Under the adjusted NucleoProbe conditions (20 nM DNA, 20 nM PM1, 12 μM MT6, and 1 nM Eu-probe) for Urine 3, we observed that EC_{50} values for Sc12 and TTFx with spiked MNase were 1.4 ± 0.4 and 2.2 ± 0.8 mU/well, respectively (Fig. 5B). No nuclease activity was detected without the MNase spiking, with any of the 1:100 diluted urine samples.

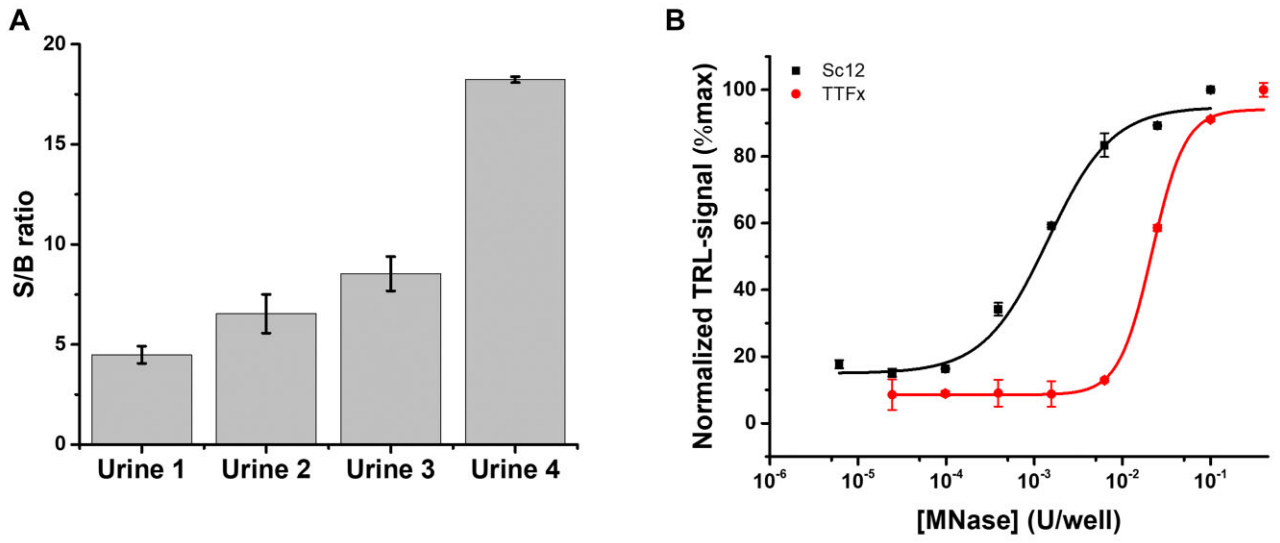

Figure 5. NucleoProbe enables nuclease activity monitoring in urine. (**A**) Urine sample (1:100) testing using Sc12 (50 nM) spiking and NucleoProbe detection (1 nM Eu-probe, 25 nM PM1, and 12 μM MT6). (**B**) Titration of Urine 3 spiked MNase (6–4000 μU) using Sc12 and TTFx (20 nM) substrates and NucleoProbe detection (1 nM Eu-probe, 20 nM PM1, and 12 μM MT6). All data were displayed as mean ± SD.

Discussion

Traditional nuclease activity assays are often designed for a specific set of nucleases, lacking universality and free selection of the used substrate nucleic acid. Recent advancements in the field have led to fast and low-cost methods with increased sensitivity (Supplementary Table S2), but there are still some disadvantages in these assays, such as substrate labeling requirements [22, 42]. Label-free methods often rely on nanoparticles that offer easy-to-use and inexpensive assays, but might limit their usage in a wide range of applications [43–45]. Especially in the case of commercial kits, the assay substrate is often unknown, and thus its usability to a certain need might be difficult to estimate beforehand. The lack of free selection of nuclease, conditions, and substrate limits the flexibility and universality, which in most cases would be desirable parameters (Supplementary Tables S1 and S2) [12].

The Protein-Probe technique, previously developed by us, has demonstrated broad applicability for a wide range of protein targets. Here, we demonstrate that by selecting a new negative (MT6) and adding a positive (PM1) modulator (Supplementary Figs S1–S4), a similar strategy can be applied to nucleic acids (Fig. 1) [34–36]. The NucleoProbe introduced here can be used for universal, label-free, and substrate sequence-independent detection of oligonucleotides and nuclease activity.

To demonstrate the capabilities of the NucleoProbe, we first showed that oligonucleotides with lengths from 9 to 60 nt can be nearly equally detected at low nanomolar concentration (Fig. 2A and B). Based on these results, 10 nM oligonucleotide concentration was selected for nearly all future assays mainly performed with 12 nt DNA. Based on the results, NucleoProbe functionality is universal, as both ss- and ds-DNA are equally detected in a sequence-independent manner (Fig. 2C and D). Additionally, DNA and RNA of the same length (12 nt) and tested modified oligonucleotides are as detectable as DNA (Supplementary Figs S9 and S11). We further used HindIII as our model restriction enzyme, to confirm the minimum oligonucleotide length demanded by the NucleoProbe. Result matches the titration of oligonucleotides (Figs 2A and 3B, and Supplementary Fig. S6). Our results show that the activity of HindIII with 9 nt substrate is detectable, as the lengths of the formed residues are 6 and 7 nt, which are not detected at low nanomolar concentrations (Fig. 2A and Supplementary S6). On the other hand, HindIII activity with 12 nt substrate was undetectable, as the lengths of the two formed residues are 7 and 9 nt, from which the 9 nt fragment is still equally detectable as the original 12 nt substrate (Fig. 2A and Supplementary Fig. S6).

We further proved the concept functionality with several DNA nucleases. Assays with three endonucleases (MNase, DNase I, and S1) and one exonuclease (Exo III), confirmed that the activity of different types of nucleases can be detected in a universal and nuclease buffer-independent manner (Fig. 3A). In addition to DNA, NucleoProbe supports the use of RNA substrates and monitoring their cleavage, as shown with RNase I and RNase A (Supplementary Figs S9 and S10). NucleoProbe was shown to tolerate at least 3 mM $ZnCl_2$, 5 mM $MgCl_2$, 5 mM $CaCl_2$, 50 mM KCl, and 100 mM NaCl without compromising functionality, covering and exceeding the typically used range of ions to enable nuclease activity. In all assays, substrate oligonucleotide was incubated with the nuclease in a buffer condition mandatory for the nuclease activity, and prior to the addition of detection components that were always added in a nuclease reaction-independent fashion. We used no additional nuclease reaction termination step, but due to the low pH in the DS buffer, nuclease activity was expected to be significantly reduced, except for S1, preferring low pH. However, the termination step can be added to the protocol simply by introducing the stop reagent together with the PM1 addition.

It was also shown that by using nonoptimal reaction components, e.g. Ca^{2+}-ion chelation with EDTA for MNase, ds-DNA substrate for Exo I, or ssDNA substrate for Exo III, the reaction rate was significantly reduced (Fig. 3C and Supplementary Fig. S7). MNase Ca^{2+} dependency was clearly visible in the NucleoProbe assay, as the high MNase activity was detected only in the presence of 1 mM Ca^{2+}, similar to

previous reports (Supplementary Fig. S7) [40, 46, 47]. Similarly, Exo I showed activity only with ssDNA and Exo III with dsDNA, as both selectively cleave only single-stranded and double-stranded oligonucleotides, by removing nucleotides in the 3′ to 5′ direction (Fig. 3C). The EC_{50} value of Exo I and Exo III shifted in relation to the length of the substrate. As the substrate with a single cleavage site was not used, a higher number of individual cleavage events is needed to "hide" the shortened substrate product from the NucleoProbe detection. This is especially important in the case of Exo III, as the substrate length must be shortened from 12 nt to at most 8 nt to be detected by the assay (Fig. 2A). Based on our observations related to nucleotide length, the highest exonuclease sensitivity would be reached by using 8 or 9 nt substrate, potentially enabling the detection of a single cleavage event (Fig. 2A). We also showed that the activity of Exo I is inhibited by capping the 3′ termini (Supplementary Fig. S8). MNase degrades the DNA with and without capping at the same rate, while Exo I cannot degrade the 3′-biotin-capped DNA, but degrades the DNA with a free 3′ terminal OH group.

To prove the exceptional sensitivity and wider suitability of the NucleoProbe, a comparative study with a commercial DD Kit (Jena Bioscience) based on FAM–substrate conjugate was performed (Fig. 3D). By using DNase I and MNase as our model enzymes, we determined 3.6 and 8.3 times lower EC_{50} values for NucleoProbe than with the DD Kit, respectively. With both methods, the activity of MNase was detectable at a lower concentration compared to DNase I, demonstrating consistency between methods, but also highlighting the high sensitivity of the NucleoProbe (Fig. 3D and Supplementary Table S2).

As assays are not always performed in pure buffer conditions, the method must tolerate some matrix components. We observed that some of these matrix effects are evaded by adjusting the concentrations of the NucleoProbe detection components. This was studied first by using bacterial cultures in TSB media, which showed a clear NucleoProbe TRL-signal quenching. This effect could be balanced out by doubling PM1 (10 nM) and lowering MT6 (5 μM) concentrations. In the case of rich culture media like TSB, also 1:400 dilution was found to be necessary for the efficient use of the NucleoProbe technique (Fig. 4A). The NucleoProbe specificity is still preserved, as shown with specific detection of *S. aureus* secreted MNase activity by using engineered TTFx and FxTT (11 nt) substrates (Fig. 4) [29, 37]. These oligonucleotides were designed with the following features: (i) increased stability against degradation by most nucleases due to the chemical modification used, 2′-*O*-methyl uridine, flanking the sequences; (ii) a single deoxy-DNA cleavage site (dT–dT) recognized by MNase; and (iii) incorporation of Fx, a nucleoside analogue used in cancer treatment that also has antibacterial activity against *S. aureus*. However, its antibacterial and therapeutic properties are not the focus of this study [37, 48]. We selected TTFx system together with its variants, including FxTT, in which Fx is positioned before the TT core, and Fx Control as a TT-free control. These substrates showed slightly higher visibility in the NucleoProbe assay compared to unmodified DNA (Sc12), but similar performance was observed in nuclease activity assays when 1:400 diluted TSB was spiked with MNase (Fig. 4B and Supplementary Fig. S11). Moreover, bacterial supernatants of. *S. epidermidis* and *E. coli* showed no activity with the TTFx substrate, as only the supernatant from the *S. aureus* culture increased the TRL signal (Fig. 4C and D) [37]. The presence of the nucleases in all supernatants was confirmed by using Sc12 and titration of the supernatants, confirming the MNase specificity (Supplementary Fig. S12). When the assay with three bacterial strains and four substrates was performed to obtain more detailed information, the correct functionality of the NucleoProbe technique became evident (Fig. 4D). In these conditions, Sc12 DNA (positive control) was efficiently cleaved by nucleases derived from all supernatants, as Fx Control (negative control) was preserved intact in all cases. MNase-specific TTFx and FxTT were cleaved only in *S. aureus* supernatants, while TTFx and FxTT stayed intact in *S. epidermidis* and *E. coli* supernatants (Fig. 4D). Results were further confirmed in Ca^{2+}-ion chelating conditions, showing MNase Ca^{2+} dependency, but also non-metal-catalyzed function of other nucleases present (Supplementary Fig. S13). It is worth mentioning that while the results with the NucleoProbe were highly similar compared to the previously reported FRET-based technique used for the original selection of the MNase-specific substrates [37], the substrate and supernatant concentrations are nearly three orders of magnitude lower, further highlighting the sensitivity of the NucleoProbe technique.

Finally, we briefly assessed the applicability of the NucleoProbe technique in urine, keeping in mind its possible usability for nuclease-based bacterial identification in the future. As the NucleoProbe is inherently nonspecific, it is not designed as a clinical method as such, but for research purposes. Expectedly, we saw that as the urine composition from different individuals varied, the NucleoProbe functionality was also differently affected. By adopting the DS composition and substrate oligonucleotide concentration with the 1:100 urine dilution, this effect could be mainly circumvented, and sufficient S/B ratios were obtained (Fig. 5A). Importantly, all four samples enabled oligonucleotide detection, and based on further MNase activity results performed with one spiked urine, nuclease activity was also sensitively monitored with the same pattern of activity for Sc12 and TTFx substrate as in the spiked TSB (Figs 4B and 5B). However, the need for assay adjustment for each urine sample individually makes the NucleoProbe tedious to use and clearly prevents its diagnostic use as such.

In conclusion, NucleoProbe provides a universal and highly sensitive platform for both endo- and exonuclease activity monitoring across diverse complex environments. Its substrate-independent and label-free design holds promises for the method's wide applicability, also beyond oligonucleotide concentration and nuclease activity monitoring. For example, NucleoProbe potentially enables the study with other DNA/RNA processing enzymes or the stability monitoring of modified oligonucleotides aimed to be used in biomedical applications. However, further studies to explore the technique in biological fluids such as blood and human serum, are yet to be performed. However, to enable clinical use, the method needs to be redesigned to increase the robustness in varying biological assay matrixes.

Acknowledgements

We would like to thank Elsi Pulkkinen and Meri Lindqvist (Department of Biology, University of Turku), for their assistance with providing HindIII.

Author contributions: Conceptualization, K.K. and H.H.; methodology, K.K. and H.H.; investigation, N.G. and B.A.B.; resources, K.K., H.H. and F.J.H.; writing original draft preparation, N.G., B.A.B., K.K., H.H., and F.J.H.; editing the

manuscript, K.K., F.J.H, and N.G.; and supervision, K.K., H.H., and F.J.H. All authors have read and agreed to published version of the manuscript.

Supplementary data

Supplementary data is available at NAR online.

Conflict of interest

Harri Härmä has commercial interest through QRET Technologies Ltd.

Funding

This work was supported by University of Turku Graduate School, Turku University Foundation (081615), Research Council of Finland (323433/K.K., 329012/K.K., and 353324/K.K.), Swedish Research Council (2021-05641), and HORIZON-MSCA-2022-COFUND-101126600-SmartBRAIN3 (F.J.H.). Funding to pay the Open Access publication charges for this article was provided by University of Turku.

Data availability

The data underlying this article are available in the article and in its online supplementary material.

References

1. Roth SB, Jalava J, Ruuskanen O *et al.* Use of an oligonucleotide array for laboratory diagnosis of bacteria responsible for acute upper respiratory infections. *J Clin Microbiol* 2004;**42**:4268–74. https://doi.org/10.1128/JCM.42.9.4268-4274.2004
2. Egli M, Manoharan M. Chemistry, structure and function of approved oligonucleotide therapeutics. *Nucleic Acids Res* 2023;**51**:2529–73. https://doi.org/10.1093/nar/gkad067
3. Roberts TC, Langer R, Wood MJA. Advances in oligonucleotide drug delivery. *Nat Rev Drug Discov* 2020;**19**:673–94. https://doi.org/10.1038/s41573-020-0075-7
4. Talap J, Zhao J, Shen M *et al.* Recent advances in therapeutic nucleic acids and their analytical methods. *J Pharm Biomed Anal* 2021;**206**:114368. https://doi.org/10.1016/j.jpba.2021.114368
5. Kulkarni JA, Witzigmann D, Thomson SB *et al.* The current landscape of nucleic acid therapeutics. *Nat Nanotechnol* 2021;**16**:630–43. https://doi.org/10.1038/s41565-021-00898-0
6. Crooke ST. Progress toward oligonucleotide therapeutics: pharmacodynamic properties. *FASEB J* 1993;**7**:533–9. https://doi.org/10.1096/fasebj.7.6.7682523
7. Sato S, Takenaka S. Highly sensitive nuclease assays based on chemically modified DNA or RNA. *Sensors* 2014;**14**:12437–50. https://doi.org/10.3390/s140712437
8. Goikoetxea G, Akhtar KTK, Prysiazhniuk A *et al.* Fluorescent and electrochemical detection of nuclease activity associated with *Streptococcus pneumoniae* using specific oligonucleotide probes. *Analyst* 2024;**149**:1289–96. https://doi.org/10.1039/D3AN01532G
9. Agrawal N, Dasaradhi PVN, Mohmmed A *et al.* RNA interference: biology, mechanism, and applications. *Microbiol Mol Biol Rev* 2003;**67**:657–85. https://doi.org/10.1128/MMBR.67.4.657-685.2003
10. Balian A, Hernandez FJ. Nucleases as molecular targets for cancer diagnosis. *Biomark Res* 2021;**9**:86. https://doi.org/10.1186/s40364-021-00342-4
11. Yang W. Nucleases: diversity of structure, function and mechanism. *Q Rev Biophys* 2011;**44**:1–93. https://doi.org/10.1017/S0033583510000181
12. Garcia Gonzalez J, Hernandez FJ. Nuclease activity: an exploitable biomarker in bacterial infections. *Expert Rev Mol Diagn* 2022;**22**:265–94. https://doi.org/10.1080/14737159.2022.2049249
13. Hernandez FJ. Nucleases: from primitive immune defenders to modern biotechnology tools. *Immunology* 2025;**174**:279–86. https://doi.org/10.1111/imm.13884
14. Killeen AA. Quantification of nucleic acids. *Clin Lab Med* 1997;**17**:1–19. https://doi.org/10.1016/S0272-2712(18)30228-2
15. Lie YS, Petropoulos CJ. Advances in quantitative PCR technology: 5′ nuclease assays. *Curr Opin Biotechnol* 1998;**9**:43–8. https://doi.org/10.1016/S0958-1669(98)80082-7
16. Norton DM, Batt AC. Detection of viable listeria monocytogenes with a 5′ nuclease PCR assay. *Appl Environ Microbiol* 1999;**65**:2122–7. https://doi.org/10.1128/AEM.65.5.2122-2127.1999
17. Cason C, D'Accolti M, Soffritti I *et al.* Next-generation sequencing and PCR technologies in monitoring the hospital microbiome and its drug resistance. *Front Microbiol* 2022;**13**:969863.
18. Le Meur J, Menut D, Wodling P *et al.* First improvements in the detection and quantification of label-free nucleic acids by laser-induced breakdown spectroscopy: application to the deoxyribonucleic acid micro-array technology. *Spectrochim Acta Part B At Spectrosc* 2008;**63**:465–73. https://doi.org/10.1016/j.sab.2007.12.011
19. Peng Z, Li J, Li S *et al.* Quantification of nucleic acid concentration in the nanoparticle or polymer conjugates using circular dichroism spectroscopy. *Anal Chem* 2018;**90**:2255–62. https://doi.org/10.1021/acs.analchem.7b04621
20. Porterfield JZ, Zlotnick A. A simple and general method for determining the protein and nucleic acid content of viruses by UV absorbance. *Virology* 2010;**407**:281–8. https://doi.org/10.1016/j.virol.2010.08.015
21. Teare JM, Islam R, Flanagan R *et al.* Measurement of nucleic acid concentrations using the DyNA Quant™ and the GeneQuant™. *BioTechniques* 1997;**22**:1170–4. https://doi.org/10.2144/97226pf02
22. Sheppard EC, Rogers S, Harmer NJ *et al.* A universal fluorescence-based toolkit for real-time quantification of DNA and RNA nuclease activity. *Sci Rep* 2019;**9**:8853. https://doi.org/10.1038/s41598-019-45356-z
23. Li Z, Zhang P, Yang B *et al.* High throughput DNA concentration determination system based on fluorescence technology. *Sens Actuators B Chem* 2021;**328**:128904. https://doi.org/10.1016/j.snb.2020.128904
24. Ponti G, Maccaferri M, Manfredini M *et al.* The value of fluorimetry (Qubit) and spectrophotometry (NanoDrop) in the quantification of cell-free DNA (cfDNA) in malignant melanoma and prostate cancer patients. *Clin Chim Acta* 2018;**479**:14–9. https://doi.org/10.1016/j.cca.2018.01.007
25. Landolt L, Marti HP, Beisland C *et al.* RNA extraction for RNA sequencing of archival renal tissues. *Scand J Clin Lab Invest* 2016;**76**:426–34. https://doi.org/10.1080/00365513.2016.1177660
26. Li X, Mauro M, Williams Z. Comparison of plasma extracellular RNA isolation kits reveals kit-dependent biases. *BioTechniques* 2015;**59**:13–7. https://doi.org/10.2144/000114306
27. Mozioğlu E, Akgoz M, Kocagöz T *et al.* Detection of nuclease activity using a simple fluorescence based biosensor. *Anal Methods* 2016;**8**:4017–21.
28. Hu J, Li WC, Qiu JG *et al.* A multifunctional DNA nanostructure based on multicolor FRET for nuclease activity assay. *Analyst* 2020;**145**:6054–60. https://doi.org/10.1039/D0AN01212B
29. Nazarenko I, Pires R, Lowe B *et al.* Effect of primary and secondary structure of oligodeoxyribonucleotides on the fluorescent properties of conjugated dyes. *Nucleic Acids Res* 2002;**30**:2089–195. https://doi.org/10.1093/nar/30.9.2089

30. Van der Gucht M, Aktan MK, Hendrix H *et al.* qDNase assay: a quantitative method for real-time assessment of DNase activity on coated surfaces. *Biochem Biophys Res Commun* 2021;**534**:1003–6. https://doi.org/10.1016/j.bbrc.2020.10.050
31. Steinek C, Guirao-Ortiz M, Stumberger G *et al.* Generation of densely labeled oligonucleotides for the detection of small genomic elements. *Cell Rep Methods* 2024;**4**:100840.
32. Takemura Y, Sekiguchi Y, Syutsubo K *et al.* Sequence-specific capture of oligonucleotide probes (SCOPE): a simple and rapid microbial rRNA quantification method using a molecular weight cutoff membrane. *Appl Environ Microbiol* 2021;**87**:e01167–21. https://doi.org/10.1128/AEM.01167-21
33. Pihlasalo S, Mariani L, Härmä H. Quantitative and discriminative analysis of nucleic acid samples using luminometric nonspecific nanoparticle methods. *Nanoscale* 2016;**8**:5902–11. https://doi.org/10.1039/C5NR09252C
34. Vuorinen E, Valtonen S, Eskonen V *et al.* Sensitive label-free thermal stability assay for protein denaturation and protein–ligand interaction studies. *Anal Chem* 2020;**92**:3512–6. https://doi.org/10.1021/acs.analchem.9b05712
35. Valtonen S, Vuorinen E, Kariniemi T *et al.* Nanomolar protein–protein interaction monitoring with a label-free protein-probe technique. *Anal Chem* 2020;**92**:15781–8. https://doi.org/10.1021/acs.analchem.0c02823
36. Vuorinen E, Valtonen S, Hassan N *et al.* Protease substrate-independent universal assay for monitoring digestion of native unmodified proteins. *Int J Mol Sci* 2021;**22**: 6362. https://doi.org/10.3390/ijms22126362
37. Borsa BA, Hernandez LI, Jiménez T *et al.* Therapeutic-oligonucleotides activated by nucleases (TOUCAN): a nanocarrier system for the specific delivery of clinical nucleoside analogues. *J Controlled Release* 2023;**361**:260–9. https://doi.org/10.1016/j.jconrel.2023.07.057
38. Vairamani M, Gross ML. G-quadruplex formation of thrombin-binding aptamer detected by electrospray ionization mass spectrometry. *J Am Chem Soc* 2003;**125**:42–3. https://doi.org/10.1021/ja0284299
39. Nagatoishi S, Isono N, Tsumoto K *et al.* Loop residues of thrombin-binding DNA aptamer impact G-quadruplex stability and thrombin binding. *Biochimie* 2011;**93**:1231–8. https://doi.org/10.1016/j.biochi.2011.03.013
40. Heins JN, Suriano JR, Taniuchi H *et al.* Characterization of a nuclease produced by *Staphylococcus aureus*. *J Biol Chem* 1967;**242**:1016–20. https://doi.org/10.1016/S0021-9258(18)96225-3
41. Kiedrowski MR, Crosby HA, Hernandez FJ *et al. Staphylococcus aureus* Nuc2 is a functional, surface-attached extracellular nuclease. *PLoS One* 2014;**9**:e95574. https://doi.org/10.1371/journal.pone.0095574
42. Mason PA, Boubriak I, Cox LS. A fluorescence-based exonuclease assay to characterize DmWRNexo, orthologue of human progeroid WRN exonuclease, and its application to other nucleases. *J Vis Exp* 2013;**82**:e50722.
43. Sanromán-Iglesias M, Garrido V, Gil-Ramírez Y *et al.* Plasmon-assisted fast colorimetric detection of bacterial nucleases in food samples. *Sens Actuators B Chem* 2021;**349**:130780. https://doi.org/10.1016/j.snb.2021.130780
44. Qing Z, He X, Qing T *et al.* Poly(thymine)-templated fluorescent copper nanoparticles for ultrasensitive label-free nuclease assay and its inhibitors screening. *Anal Chem* 2013;**85**:12138–43. https://doi.org/10.1021/ac403354c
45. Liu R, Hu J, Chen Y *et al.* Label-free nuclease assay with long-term stability. *Anal Chem* 2019;**91**:8691–6. https://doi.org/10.1021/acs.analchem.9b02467
46. von Hippel PH, Felsenfeld G. Micrococcal nuclease as a probe of DNA conformation. *Biochemistry* 1964;**3**:27–39. https://doi.org/10.1021/bi00889a006
47. Tiet P, Clark KC, McNamara II JO *et al.* Colorimetric detection of *Staphylococcus aureus* contaminated solutions without purification. *Bioconjug Chem* 2017;**28**:183–93. https://doi.org/10.1021/acs.bioconjchem.6b00571
48. Thomson JM, Lamont IL. Nucleoside analogues as antibacterial agents. *Front Microbiol* 2019;**10**:952.

Received: March 12, 2025. **Revised:** August 17, 2025. **Accepted:** August 19, 2025